Acta Crystallographica Section F
**Structural Biology and Crystallization Communications**
ISSN 1744-3091

# Crystallization, preliminary X-ray diffraction studies and Raman microscopy of the major haemoglobin from the sub-Antarctic fish *Eleginops maclovinus* in the carbomonoxy form

**Antonello Merlino,[a,b] Luigi Vitagliano,[b] Anna Balsamo,[a] Francesco P. Nicoletti,[c] Barry D. Howes,[c] Daniela Giordano,[d] Daniela Coppola,[d] Guido di Prisco,[d] Cinzia Verde,[d] Giulietta Smulevich,[c] Lelio Mazzarella[a,b] and Alessandro Vergara[a,b]***

[a]Department of Chemistry, University of Naples 'Federico II', 80126 Naples, Italy, [b]Istituto di Biostrutture e Bioimmagini, CNR, 80134 Naples, Italy, [c]Department of Chemistry 'Ugo Schiff', University of Florence, 50019 Sesto Fiorentino (FI), Italy, and [d]Institute of Protein Biochemistry, CNR, 80131 Naples, Italy

Correspondence e-mail: avergara@unina.it

Received 16 June 2010
Accepted 27 September 2010



The blood of the sub-Antarctic fish *Eleginops maclovinus* (Em) contains three haemoglobins. The major haemoglobin (Hb1Em) displays the Root effect, a drastic decrease in the oxygen affinity and a loss of cooperativity at acidic pH. The carbomonoxy form of HbEm1 has been crystallized in two different crystal forms, orthorhombic (Ortho) and hexagonal (Hexa), and high-resolution diffraction data have been collected for both forms (1.45 and 1.49 Å resolution, respectively). The high-frequency resonance Raman spectra collected from the two crystal forms using excitation at 514 nm were almost indistinguishable. Hb1Em is the first sub-Antarctic fish Hb to be crystallized and its structural characterization will shed light on the molecular mechanisms of cold adaptation and the role of the Root effect in fish haemoglobins.

## 1. Introduction

Fish haemoglobins (Hbs) have been extensively studied not only to determine their structural and functional properties (Perutz, 1990), but also because they offer the possibility of investigating functional differentiation and molecular adaptation in species living in a large variety of environmental conditions. As in mammals, fish Hb is a heterotetramer. Much of our knowledge of the effect of the environment on vertebrate physiology and evolution comes from the study of fishes, which share most physiological mechanisms with mammals (Bonaventura *et al.*, 2004). Their bodies are submerged in water and their close physical and physiological relationship with the aquatic environment makes them sensitive sentinels of environmental challenge and offers important advantages in defining the organism–environment interface and responses to temperature adaptation (Verde *et al.*, 2007). The Antarctic notothenioids, including high-Antarctic, sub-Antarctic and temperate species, provide many opportunities for comparative approaches aimed at understanding protein thermal adaptations and their ability to counteract ongoing climate change (Verde *et al.*, 2008).

In addition to being highly sensitive to pH, several fish Hbs also become non-cooperative at acidic pH. The complete loss of cooperativity (indicated by a Hill coefficient of 1) and the inability to saturate the ligand sites at low pH values, even at high oxygen pressure, that are common to many fish Hbs are distinctive properties with respect to the Bohr effect and are known as the Root effect (Brittain, 2005).

Structural studies of Hbs from several temperate fish [tuna (Yokoyama *et al.*, 2004), spot (Mylvaganam *et al.*, 1996) and trout (Tame *et al.*, 1996)] displaying the Root effect have been conducted in their ferrous form. Furthermore, several high-Antarctic fish Hbs have been crystallized in both ferrous and ferric forms and their crystal structures have been determined (Camardella *et al.*, 1992; Ito *et al.*, 1995; Mazzarella, Bonomi *et al.*, 2006; Mazzarella *et al.*, 1999; Mazzarella, Vergara *et al.*, 2006; Vergara *et al.*, 2007, 2009, 2010; Merlino *et al.*, 2009; Vitagliano *et al.*, 2004, 2008; Riccio *et al.*, 2002). In particular, Hbs from *Trematomus bernacchii* (HbTb; Ito *et al.*, 1995; Mazzarella, Bonomi *et al.*, 2006; Mazzarella, Vergara *et al.*, 2006) and

*T. newnesi* (the major, Hb1Tn, and the cathodic, HbCTn, component; Mazzarella, Bonomi *et al.*, 2006; Mazzarella *et al.*, 1999; Vergara *et al.*, 2010) have been studied in their ferrous form. These studies have provided several possible structural explanations of the Root effect. The autoxidation process of Antarctic fish Hbs was extensively investigated in HbTb (Merlino *et al.*, 2009; Vitagliano *et al.*, 2004) and Hb1Tn (Vitagliano *et al.*, 2008), revealing the accessibility of a quaternary structure different from the canonical R and T states. In particular, the ferric states of HbTb (Vergara *et al.*, 2007) and Hb1Tn (Riccio *et al.*, 2002) are able to form an intermediate R/T state. In addition, it is noted that the Root effect can also affect the quaternary structure of the ferric state at acidic pH (Vergara *et al.*, 2009).

*E. maclovinus*, locally known as mullet or róbalo, is a notothenioid belonging to the family Eleginopidae and is the only species of its genus. It is an important component of the ichthyofauna in the coastal temperate and sub-Antarctic waters of South America; it is also found in coastal waters around the Falkland Islands (Brickle *et al.*, 2005). *E. maclovinus* forms a sister group of Antarctic notothenioids that dominate the cold-shelf waters of Antarctica and represents the 'starting point' for notothenioid radiation (Eastman & Lannoo, 2008).

Ion-exchange chromatography of the haemolysate of *E. maclovinus* shows the presence of three components (HbCEm, Hb1Em and Hb2Em; Coppola *et al.*, 2010). We studied the major component Hb1Em, a tetrameric Hb that displays the Root effect. Sequence alignments show a significant similarity to high-Antarctic fish Hbs. Indeed, Hb1Em shares 85% sequence identity to HbTb (Camardella *et al.*, 1992), the carbomonoxy (Camardella *et al.*, 1992) and deoxy (Ito *et al.*, 1995; Mazzarella *et al.*, 2006) structures of which have previously been determined. *T. bernacchii* is an Antarctic notothenioid living at 271 K, whereas *E. maclovinus* is a sub-Antarctic notothenioid adapted to 278–288 K. *E. maclovinus* essentially never experiences near-freezing water temperatures and the absence of a nucleotide sequence coding for antifreeze glycoproteins (AFGPs) in this fish supports this scenario (Cheng *et al.*, 2003).

Therefore, with the aim of obtaining insight into the mechanism of Hb cold adaptation and to understand the structural basis of the Root effect at low temperatures, we have undertaken the structural characterization of Hbs isolated from sub-Antarctic fishes. Here, we report the crystallization, Raman microscopy and preliminary diffraction studies of Hb1Em in the carbomonoxy form (Hb1EmCO).

## 2. Methods

### 2.1. Collection of specimens and purification

Specimens of *E. maclovinus* were collected during the ICEFISH 2004 cruise. Adult *E. maclovinus* were collected near the Falkland Islands. Blood was taken from the caudal vein using heparinized syringes. Haemolysates were prepared as described previously (D'Avino & Prisco, 1988). Saline-washed erythrocytes were frozen at 193 K until use.

Separation of *E. maclovinus* Hbs was achieved by FPLC anion-exchange chromatography on a Mono Q-Tricorn column (1.0 × 10 cm) equilibrated with 20 m*M* Tris–HCl pH 7.6 (buffer *A*). Elution was performed with a gradient from buffer *A* to 20 m*M* Tris–HCl pH 7.6, 100 m*M* NaCl (buffer *B*). A mixture of HbC and Hb1 was eluted at 50% buffer *B*, Hb1 was eluted at 57% buffer *B* and a mixture of Hb1 and Hb2 was eluted at 60% buffer *B* (Supplementary Fig. S1[1]). Hb1Em was further purified by ion-exchange chromatography on a DE52 column equilibrated with 10 m*M* Tris–HCl pH 7.6 and eluted stepwise with the same buffer. All steps were carried out at 273–278 K (Brickle *et al.*, 2005; Coppola *et al.*, 2010).

### 2.2. Crystallization

Hb1Em stock solutions were kept in the carbomonoxy form. The formation of the carbomonoxy form was monitored by optical spectroscopy. Crystallization trials were performed at 277 K in a CO atmosphere provided by flushing the gas in the flask containing the crystallization reactors. Crystals were obtained using the dialysis technique with microdialysis buttons. In buttons in which crystallization had occurred, crystals with different crystal habits were observed.

Crystals of the ferric form were prepared for resonance Raman experiments starting from carbomonoxy crystals by soaking a stabilizing solution containing 10 m*M* potassium ferricyanide into the crystals and then washing the excess off with stabilizing solution. The deoxy Hb crystals were obtained by treating crystals of the ferric form with degassed stabilizing solutions containing 10 m*M* sodium dithionite.

### 2.3. Data collection and processing

X-ray diffraction data were collected both in-house using a Rigaku MicroMax-007 HF generator equipped with a Saturn944 CCD detector and at the ELETTRA synchrotron. Cryoconditions for diffraction at 100 K were provided by the addition of 20% glycerol to the harvesting solution. Independent resonance Raman control experiments indicated that it was necessary to add 10 m*M* sodium dithionite to the harvesting and cryoprotecting solutions in order to avoid oxidation.

Diffraction data from the two different crystal forms were collected. In both cases, the oscillation range per image was 0.5°. The exposure time per image was 50 s for the data collected in-house and 20 s for the synchrotron data. Reflections were indexed, integrated and scaled using the *HKL*-2000 package (Otwinowski & Minor, 1997). The precision-indicating merging *R* factors ($R_{\rm p.i.m.}$) were calculated using the program *RMERGE* (Weiss, 2001; Evans, 2006).

### 2.4. Structure determination

Determination of the crystal structure was performed by molecular replacement using the program *AMoRe* (Navaza & Saludjian, 1997). HbTb (PDB code 3gkv; Merlino *et al.*, 2009), with which Hb1Em shares 85% sequence identity, was used as a search model.

### 2.5. Raman microscopy

During most of the analysis, crystals were kept in a 1 µl drop of mother liquor. Crystals were transferred from plates to a single hanging-drop reactor and then analyzed on a Raman microscope apparatus consisting of a confocal Raman instrument (Jasco NRS-3100) equipped with an Olympus microscope. Resonance Raman (RR) spectra were obtained at room temperature with the 514.5 nm line of an air-cooled $Ar^+$ laser (Melles Griot) focused to a spot size of approximately 4 µm by a 20× objective. A holographic notch filter was used to reject the excitation laser line from the scattered light. Raman scattering was dispersed through a monochromator (1200 grooves $mm^{-1}$ grating) and collected using a Peltier-cooled 1024 × 128 pixel CCD photon detector (Andor DU401BVI). Typically, several 2 min spectra (7 $cm^{-1}$ resolution) were recorded and averaged using a standard software routine. The RR spectra were

[1] Supplementary material has been deposited in the IUCr electronic archive (Reference: RP5054).

calibrated using indene as a standard. The frequencies were accurate to within 1 $cm^{-1}$ for the intense isolated bands and to about 2 $cm^{-1}$ for overlapped bands or shoulders. The laser power at the crystal was 1–2 mW for the ferric and deoxy forms and 0.1 mW for the carbomonoxy form (in order to avoid photolysis).

## 3. Results and discussion

Initial screenings for Hb1EmCO crystallization were conducted in dialysis buttons using the ammonium sulfate solutions that yielded crystals of the major Hb component of *T. newnesi* (Mazzarella *et al.*, 1999). 10 µl protein solution at 20 mg $ml^{-1}$ in 100 m*M* Tris–HCl buffer pH 8.0 and 2 m*M* sodium dithionite was dialyzed against a 25 ml reservoir containing 2 *M* ammonium sulfate, 100 m*M* Tris–HCl pH 8.0 and 2 m*M* sodium dithionite. The quality of the crystals was then improved by fine-tuning the sulfate concentration. The best crystals were obtained in a week using 20 mg $ml^{-1}$ Hb1Em and 1.8 *M* ammonium sulfate. In the same flask, different dialysis buttons contained crystals displaying two different morphologies (bipyramidal and rod-like).

Diffraction data (Fig. 1) were collected for the two types of Hb1EmCO crystals: Ortho (rod-like crystals) and Hexa (bipyramidal crystals). The maximum dimensions of the Ortho crystals were 0.05 × 0.05 × 0.4 mm, whereas those of the Hexa crystals were 0.1 × 0.1 × 0.2 mm. For the rod-like crystals, in-house data collections were carried out at 298 and 100 K. Data at room temperature were collected by mounting the crystal in a capillary filled with CO, whereas the data at 100 K were collected by flash-cooling in supercooled $N_2$ produced by an Oxford Cryosystem after the addition of 20% glycerol to the harvesting solution.

Diffraction data for the crystals with bipyramidal morphology were collected at the ELETTRA synchrotron-radiation facility. Crystals were flash-cooled at 100 K after addition of 20% glycerol to the harvesting solution.

All data sets were indexed and processed with the *HKL*-2000 suite of programs. Statistics of data processing are reported in Table 1. The two crystal forms belonged to space groups $P6_122$ (Hexa) and $P2_12_12_1$ (Ortho). As frequently observed (see, for example, Tilton *et al.*, 1992; Merlino *et al.*, 2005), the X-ray data sets of the Ortho crystals at room temperature and at 100 K gave similar unit-cell parameter values. Matthews coefficient calculations suggested the presence of one $\alpha\beta$ dimer in the asymmetric unit for the Hexa crystals and one tetramer ($\alpha_2\beta_2$) in the asymmetric unit for the Ortho crystals.

The phase problem was solved by molecular replacement using the program *AMoRe* (Navaza & Saludjian, 1997) with the structure of partially oxidized HbTb (PDB code 3gkv; Merlino *et al.*, 2009) as a search model. For both crystal forms, a clear solution was easily obtained.

The preliminary electron-density maps were of excellent quality. Integrated automated and manual model-building sessions, aimed at defining the complete structures, were performed using the programs *ARP*/*wARP* (Perrakis *et al.*, 2001) and *O* (Jones *et al.*, 1990). Refinement of the structures is in progress.

Raman microscopy experiments were conducted on Hb1EmCO crystals (both Ortho and Hexa) as well as on their ferric and deoxy forms. The high-frequency region (1300–1700 $cm^{-1}$) of the RR spectrum includes the porphyrin in-plane vibrational modes (which are sensitive to the electron density of the macrocycle and the oxidation, coordination and spin state of the iron ion). High-frequency RR spectra of Hb1Em crystals of the Ortho and Hexa forms together with those of the corresponding ferric and deoxy forms obtained with 514.5 nm excitation are shown in Fig. 2. The ferric form contains a hexacoordinated low-spin haemichrome (bands at 1505, 1559, 1588 and 1640 $cm^{-1}$ assigned to $\nu_3$, $\nu_{38}$, $\nu_{19}$ and $\nu_{10}$ modes, respectively), as previously observed in HbTb crystals (Merlino, Verde *et al.*, 2008). The deoxy forms of both Ortho and Hexa are pentacoordinated high-spin states ($\nu_4$, $\nu_{19}$, $\nu_{37}$ and $\nu_{10}$ at 1355, 1548–1549, 1582 and 1602–1607 $cm^{-1}$, respectively). However, after long laser exposure times (about 10 min), the Ortho but not the Hexa form appears to be unstable under laser irradiation, since it irreversibly converts to a hexacoordinated low-spin haemochrome state (haemo, with $\nu_4$, $\nu_3$ and $\nu_{19}$ at 1361, 1496 and 1587 $cm^{-1}$, respectively).

Even at low laser power (0.1 mW), the degree of photolysis of both carbomonoxy forms of Hb1Em was high, as was apparent from the relative intensity of the $\nu_4$ bands of the CO and photolyzed species (1374 and 1355 $cm^{-1}$, respectively) and the presence of bands arising

**Table 1**
Data-collection statistics.

Values in parentheses are for the highest resolution shell.

| | Hexa, $T$ = 100 K | Ortho, $T$ = 100 K | Ortho, $T$ = 298 K |
|---|---|---|---|
| Space group | $P6_122$ | $P2_12_12_1$ | $P2_12_12_1$ |
| Unit-cell parameters | | | |
| $a$ (Å) | 91.702 | 58.175 | 58.473 |
| $b$ (Å) | 91.702 | 88.075 | 89.888 |
| $c$ (Å) | 168.716 | 123.194 | 125.278 |
| Asymmetric unit | $\alpha\beta$ dimer | $\alpha_2\beta_2$ tetramer | $\alpha_2\beta_2$ tetramer |
| Resolution range (Å) | 30–1.49 (1.53–1.49) | 50–1.45 (1.50–1.45) | 50–2.05 (2.12–2.05) |
| No. of total reflections | 212199 | 384398 | 108997 |
| No. of unique reflections | 66710 | 109738 | 40284 |
| Completeness (%) | 96.4 (92.5) | 97.3 (90.8) | 95.2 (95.2) |
| Multiplicity | 3.2 (2.6) | 3.5 (2.5) | 2.7 (2.6) |
| $R_{merge}$ (%) | 0.095 (0.440) | 0.075 (0.384) | 0.095 (0.580) |
| $I/\sigma(I)$ | 8.0 (2.1) | 37.5 (3.3) | 7.4 (2.2) |
| $R_{p.i.m.}$ (%) | 0.057 (0.295) | 0.039 (0.284) | 0.075 (0.400) |
| $B$ value from Wilson plot ($A^2$) | 23.8 | 16.1 | 34.1 |

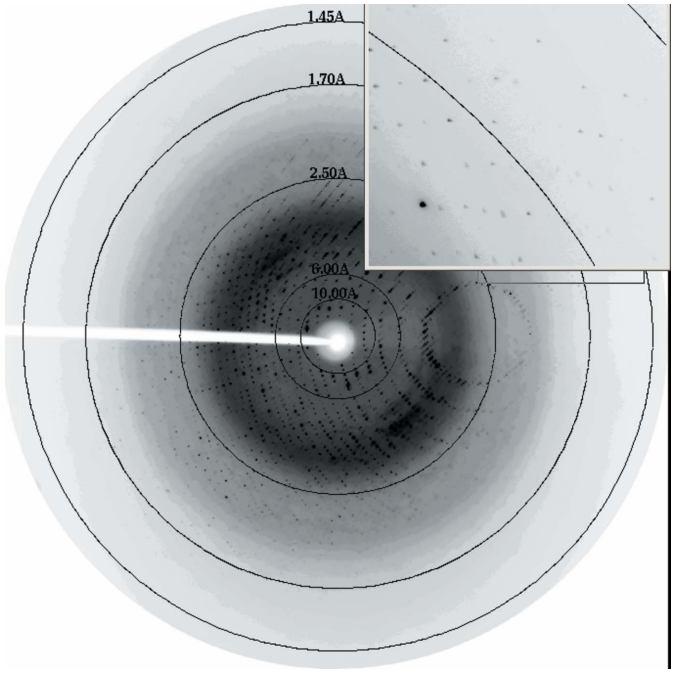


**Figure 1**
Diffraction pattern of the Hb1EmCO crystal in the Hexa form. Diffraction spots are detectable up to 1.45 Å resolution.

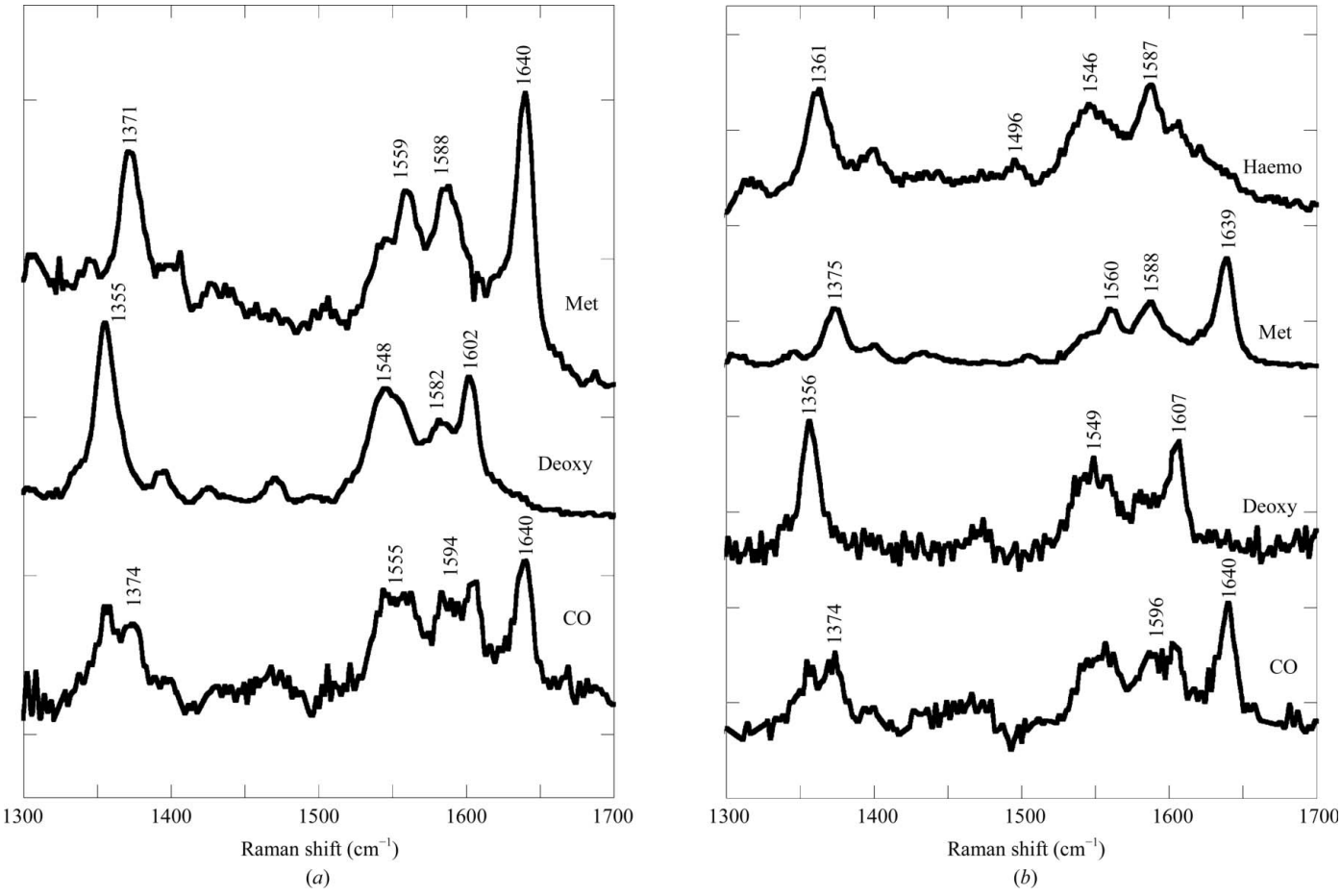


**Figure 2**
Resonance Raman spectra of crystals of Hb1Em in 100 m*M* Tris–HCl buffer pH 8.0 at room temperature in the carbomonoxy (CO), deoxygenated (Deoxy) and ferric (Met) forms for Hexa (*a*) and Ortho (*b*) crystals. The Ortho deoxygenated form (*b*) converts quickly into haemochrome (Haemo) after 10 min laser exposure. Excitation wavelength, 514.5 nm; laser power at the sample 2 mW for the ferric and deoxy forms and 0.1 mW for the carbomonoxy form. All spectra were an average of at least six spectra with 2 min integration time.

from $\nu_{19}$ and $\nu_{10}$ of both the deoxy form and the CO complex (deoxy bands at 1548–1549 and 1602–1607 cm$^{-1}$, respectively).

Raman microscopy, as previously demonstrated (Vergara *et al.*, 2008; Merlino, Verde *et al.*, 2008; Merlino, Sica *et al.*, 2008), is a valuable tool for the preliminary investigation of protein single crystals. Indeed, apart from the different stability in the laser beam, no significant difference was observed using Raman spectroscopy and the respective spectra of the two forms of Hb1Em (Hexa and Ortho) in the carbomonoxy, deoxy and ferric forms are indistinguishable within the experimental noise.

Hb1Em is the first sub-Antarctic fish Hb to be crystallized. Determination of the Hb1EmCO structure will allow detailed comparative analyses with the structures of its psychrophilic (HbTb; Merlino *et al.*, 2009) and mesophilic (tuna; Yokoyama *et al.*, 2004) counterparts. These analyses will provide insights into Root-effect adaptation at low temperature.

This work was financially supported by PNRA (Italian National Programme for Antarctic Research) and is in the framework of the programme Evolution and Biodiversity in the Antarctic (EBA) sponsored by the Scientific Committee for Antarctic Research (SCAR). This study was partially supported by the Ministero Italiano dell'Università e della Ricerca Scientifica (PRIN 2007SFZXZ7, 'Structure, function and evolution of haem proteins from Arctic and Antarctic marine organisms: cold-adaptation mechanisms and acquisition of new functions'). The ICEFISH cruise was supported by the National Science Foundation grant OPP 0132032 to H. William Detrich (Chief Scientist, Northeastern University). We thank Giosuè Sorrentino and Maurizio Amendola for their technical assistance. We thank the Elettra Synchrotron (Trieste, Italy) for beam time and the staff of the XRD1 beamline for assistance during data collection and the Consorzio Regionale di Competenze in Biotecnologie Industriali (BioTekNet) are also acknowledged.

## References

Bonaventura, C., Crumbliss, A. L. & Weber, R. E. (2004). *Acta Physiol. Scand.* **182**, 245–258.
Brickle, P., Arkhipkin, A. I. & Shcherbich, Z. N. (2005). *J. Mar. Biol. Assoc. U. K.* **85**, 1217–1221.
Brittain, T. (2005). *J. Inorg. Biochem.* **99**, 120–129.
Camardella, L., Caruso, C., D'Avino, R., di Prisco, G., Rutigliano, B., Tamburrini, M., Fermi, G. & Perutz, M. F. (1992). *J. Mol. Biol.* **224**, 449–460.
Cheng, C.-H. C., Chen, L., Near, T. & Jin, Y. (2003). *Mol. Biol. Evol.* **20**, 1897–1908.
Coppola, D., Giordano, D., Vergara, A., Mazzarella, L., di Prisco, G., Verde, C. & Russo, R. (2010). *Polar Sci.* **4**, 295–308.
D'Avino, R. & di Prisco, G. (1988). *Comp. Biochem. Physiol. B*, **90**, 579–584.
Eastman, J. T. & Lannoo, M. J. (2008). *J. Morphol.* **269**, 84–103.
Evans, P. (2006). *Acta Cryst.* D**62**, 72–82.
Ito, N., Komiyama, N. H. & Fermi, G. (1995). *J. Mol. Biol.* **250**, 648–658.

Jones, T. A., Bergdoll, M. & Kjeldgaard, M. (1990). *Crystallographic and Modelling Methods in Molecular Design*, edited by C. Bugg & S. Ealick, pp. 189–199. New York: Springer-Verlag.
Mazzarella, L., Bonomi, G., Lubrano, M. C., Merlino, A., Vergara, A., Vitagliano, L., Verde, C. & di Prisco, G. (2006). *Proteins*, **62**, 316–321.
Mazzarella, L., D'Avino, R., di Prisco, G., Savino, C., Vitagliano, L., Moody, P. C. & Zagari, A. (1999). *J. Mol. Biol.* **287**, 897–906.
Mazzarella, L., Vergara, A., Vitagliano, L., Merlino, A., Bonomi, G., Scala, S., Verde, C. & di Prisco, G. (2006). *Proteins*, **65**, 490–498.
Merlino, A., Mazzarella, L., Di Fiore, A., Carannante, A., Notomista, E., Di Donato, A. & Sica, F. (2005). *J. Biol. Chem.* **280**, 17953–17960.
Merlino, A., Sica, F., Zagari, A, Mazzarella, L. & Vergara, A. (2008). *Biophys. Chem.* **137**, 24–27.
Merlino, A., Verde, C., di Prisco, G., Mazzarella, L. & Vergara, A. (2008). *Spectroscopy*, **22**, 143–152.
Merlino, A., Vitagliano, L., Howes, B., Verde, C., di Prisco, G., Smulevich, G., Sica, F. & Vergara, A. (2009). *Biopolymers*, **91**, 1117–1125.
Mylvaganam, S. E., Bonaventura, C., Bonaventura, J. & Getzoff, E. D. (1996). *Nature Struct. Biol.* **3**, 275–283.
Navaza, J. & Saludjian, P. (1997). *Methods Enzymol.* **276**, 581–594.
Otwinowski, Z. & Minor, W. (1997). *Methods Enzymol.* **276**, 307–326.
Perrakis, A., Harkiolaki, M., Wilson, K. S. & Lamzin, V. S. (2001). *Acta Cryst.* D**57**, 1445–1450.
Perutz, M. F. (1990). *Annu. Rev. Physiol.* **52**, 1–25.
Riccio, A., Vitagliano, L., di Prisco, G., Zagari, A. & Mazzarella, L. (2002). *Proc. Natl Acad. Sci. USA*, **99**, 9801–9806.
Tame, J. R., Wilson, J. C. & Weber, R. E. (1996). *J. Mol. Biol.* **259**, 749–760.
Tilton, R., Dewan, J. C. & Petsko, G. (1992). *Biochemistry*, **31**, 2469–2481.
Verde, C., Vergara, A., Mazzarella, L. & di Prisco, G. (2008). *Curr. Protein Pept. Sci.* **9**, 578–590.
Verde, C., Vergara, A., Parisi, E., Giordano, D., Mazzarella, L. & di Prisco, G. (2007). *Antarct. Sci.* **19**, 271–278.
Vergara, A., Franzese, M., Merlino, A., Bonomi, G., Verde, C., Giordano, D., di Prisco, G., Lee, H.C., Peisach, J. & Mazzarella, L. (2009). *Biophys. J.* **97**, 866–874.
Vergara, A., Franzese, M., Merlino, A., Vitagliano, L., di Prisco, G., Verde, C., Lee, H. C., Peisach, J. & Mazzarella, L. (2007). *Biophys. J.* **93**, 2822–2829.
Vergara, A., Merlino, A., Pizzo, E., D'Alessio, G. & Mazzarella, L. (2008). *Acta Cryst.* D**64**, 167–171.
Vergara, A., Vitagliano, L., Merlino, A., di Prisco, G., Verde, C. & Mazzarella, L. (2010). *J. Biol. Chem.* **285**, 32568–32575.
Vitagliano, L., Bonomi, G., Riccio, A., di Prisco, G., Smulevich, G. & Mazzarella, L. (2004). *Eur. J. Biochem.* **271**, 1651–1659.
Vitagliano, L., Vergara, A., Bonomi, G., Merlino, A., Smulevich, G., Howes, B., di Prisco, G., Verde, C. & Mazzarella, L. (2008). *J. Am. Chem. Soc.* **130**, 10527–10535.
Weiss, M. S. (2001). *J. Appl. Cryst.* **34**, 130–135.
Yokoyama, T., Chong, K. T., Miyazaki, G., Morimoto, H., Shih, D. T. B., Unzai, S., Tame, J. R. H. & Park, S.-Y. (2004). *J. Biol. Chem.* **279**, 28632–28640.